Mechanics of Materials 75 (2014) 103–110

Contents lists available at ScienceDirect

Mechanics of Materials

journal homepage: www.elsevier.com/locate/mechmat

Fibrous composites of piezoelectric and piezomagnetic phases: Generalized plane strain with transverse electromagnetic fields

Hsin-Yi Kuo *

Department of Civil Engineering, National Chiao Tung University, Hsinchu 30010, Taiwan

ARTICLE INFO

Article history:
Received 24 January 2014
Received in revised form 7 April 2014
Available online 20 April 2014

Keywords:
Magnetoelectricity
Fibrous composite
Generalized plane strain
Transverse electromagnetic field

ABSTRACT

This work presents a theoretical framework for solving the field distributions of a piezoelectric–piezomagnetic fibrous composite subjected to generalized plane strain with transverse electromagnetic fields. The matrix is infinite containing arbitrarily distributed circular cylinders, which may have different sizes and material properties. By introducing an eigenstrain corresponding to the electro-magneto-elastic effect, this coupling problem can be reduced to an equivalent plane elasticity problem. The classic work of Muskhelishvili to obtain the elastic potential of a composite is generalized to the current multi-field multi-inclusion media. Several numerical examples are presented to demonstrate the effectiveness of the approach.

© 2014 Elsevier Ltd. All rights reserved.

1. Introduction

The magneto-electric (ME) coupling refers to the polarization induced by a magnetic field, or conversely the magnetization induced by an electric field. It was first predicted by Landau and Lifshitz (1984) and observed by Astrov (1960) and Rado and Folen (1961) over fifty years ago. This ME effect has recently drawn ever-increasing interest due to their potential applications as multifunctional devices including ME data storage and switching (Spaldin and Fiebig, 2005), modulation of optical waves (Fiebig, 2005), and electrically microwave phase shifters (Bichurin et al., 2002). However, the coupling is rather weak in a single-phase material even at low temperature, and this has motivated the study of composites of piezoelectric and piezomagnetic media. The "product property" causes the ME effect in this multiferroic composite: an applied electric field generates a deformation in the piezoelectric phase, which in turn generates a deformation in the piezomagnetic phase, resulting a magnetization (Nan et al., 2008).

The promise of applications, and the indirect coupling through strain have also made ME composites the topic of a number of theoretical investigations. Among them, Nan (1994), Srinivas and Li (2005) and Liu and Kuo (2012) estimated the effective properties of ME composites of non-dilute volume fractions by mean-field-type models. Benveniste (1995) derived exact relations in a ME composite with cylindrical geometry. The analysis for local fields is available for simple microstructures such as a single ellipsoidal inclusion (Huang and Kuo, 1997; Li and Dunn, 1998), arbitrarily distributed or periodic arrays of fibrous ME composites (Kuo, 2011; Kuo and Pan, 2011; Kuo and Bhattacharya, 2013), and laminates (Kuo et al., 2010). In addition, Liu et al. (2004) and Lee et al. (2005) used finite element method to address ME composites for general microstructures, while Aboudi (2001) and Camacho-Montes et al. (2009) adopted the homogenization method. However, much of this work uses approximate methods and models based on single inclusions to estimate the

* Tel.: +886 6 5712121 54961.
E-mail address: hykuo@mail.nctu.edu.tw

http://dx.doi.org/10.1016/j.mechmat.2014.04.007
0167-6636/© 2014 Elsevier Ltd. All rights reserved.

effective properties of composites. Exact methods that provides the detailed field distribution are limited to the medium subjected to the anti-plane shear with in-plane electromagnetic fields due to the complexity.

In a classic work, Muskhelishvili (1975) used the Kolosov–Muskhelishvili potentials with truncated Laurent series for elastic problems with circular boundaries. Analogous representations were employed by McPhedran and Movchan (1994) for a pair and a square array of circular elastic inclusions, by Buryachenko and Kushch (2006) for a matrix reinforced two linearly elastic isotropic aligned circular fibers, and by Kushch et al. (2008) for the progressive damage in the fiber reinforced composite. This method was extended to investigate the multiple piezoelectric inclusions in a non-piezoelectric matrix (Yang and Gao, 2010), and for a three-phase thermo-electro-magneto-elastic cylinder model (Tong et al., 2008). In addition, a Galerkin boundary integral method has also been developed to address the elastic composites with multiple circular cylinders (Mogilevskaya and Crouch, 2001), while Eshelby's equivalent inclusion for a fibrous piezoelectric inhomogeneity was proposed by Xiao and Bai (1999). In this paper, we generalize Muskhelishvili's methodology to a fibrous composite made of piezoelectric and piezomagnetic phases under generalized plane strain $(\varepsilon_{13}^0 = 0, \varepsilon_{23}^0 = 0, \varepsilon_{33}^0 \neq 0)$ with transverse electromagnetic fields. Specifically we seek the stress and displacement distributions of the composite.

The remainder of this paper is organized as follows. In Section 2 we formulate the equation for a piezoelectric–piezomagnetic composite under generalized plane strain with transverse electromagnetic fields. We show that the multi-field coupled problem can be reduced to an equivalent plane elastic problem with a corresponding uniform eigenstrain. In Section 3 we generalize the work of Muskhelishvili (1975) to obtain a representation of the solution. The basic idea is to express the stress and displacement via two complex potentials and expand each field in each medium in a series. We use this method to study selected systems with sufficient accuracy in Section 4.

2. General framework

Let us consider an infinite medium containing N arbitrarily distributed, parallel and separated circular cylinders (Fig. 1). The domain of the pth circular cylinder is denoted V_p, $p = 1, 2, \ldots, N$, and the remaining matrix is denoted Ω_m. We assume that the cylinders and the matrix are made of distinct phases: transversely isotropic piezoelectric or piezomagnetic materials. A global Cartesian coordinate system is introduced with x_1- and x_2-axes in the plane of the cross-section and x_3-along the axes of the cylinders (Fig. 1). The centers of the pth circular cylinder are designated as O_p, each of which may have different radii a_p.

Assume that the composite is subjected to in-plane mechanical strain ε_{11}^0, ε_{22}^0 and ε_{12}^0 (or in-plane stress σ_{11}^0, σ_{22}^0 and σ_{12}^0) at infinity and uniform strain ε_{33}^0, electric field E_3^0 and magnetic field H_3^0 in the x_3-direction. It can be shown that the general constitutive law for the non-vanishing

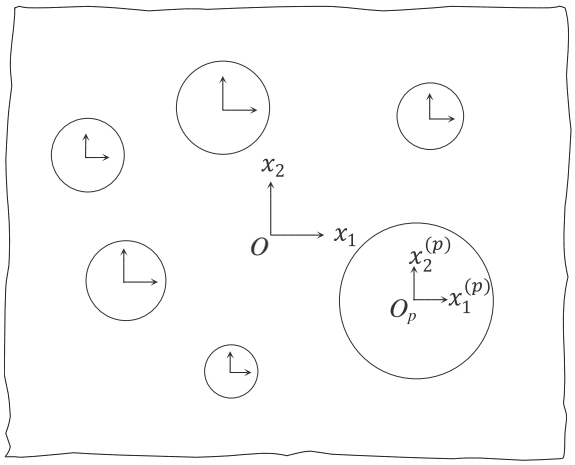

Fig. 1. The cross-section of the multiple fibers composite.

field quantities can be written in a compact form as (Benveniste, 1995)

$$\begin{pmatrix} \sigma_{11} \\ \sigma_{22} \\ \sigma_{33} \\ \sigma_{12} \\ D_3 \\ B_3 \end{pmatrix} = \begin{pmatrix} C_{11} & C_{12} & C_{13} & 0 & e_{31} & q_{31} \\ C_{12} & C_{11} & C_{13} & 0 & e_{31} & q_{31} \\ C_{13} & C_{13} & C_{33} & 0 & e_{33} & q_{33} \\ 0 & 0 & 0 & C_{66} & 0 & 0 \\ e_{31} & e_{31} & e_{33} & 0 & -\kappa_{33} & -\lambda_{33} \\ q_{31} & q_{31} & q_{33} & 0 & -\lambda_{33} & -\mu_{33} \end{pmatrix} \begin{pmatrix} \varepsilon_{11} \\ \varepsilon_{22} \\ \varepsilon_{33} \\ 2\varepsilon_{12} \\ -E_3 \\ -H_3 \end{pmatrix}. \tag{2.1}$$

Here σ_{ij} and ε_{ij} are the stress and strain; D_i and E_i are the electric displacement and electric field; B_i and H_i are the magnetic flux and magnetic field, respectively. C_{11}, C_{12}, C_{13}, C_{33}, and C_{66} are the elastic moduli, e_{31} and e_{33} are piezoelectric constants, q_{31} and q_{33} are piezomagnetic constants, and κ_{33}, μ_{33}, and λ_{33} are the dielectric permittivity, magnetic permeability and magnetoelectric coefficients, respectively.

The constitutive equation (2.1) are rather complicated. However, it is observed that ε_{33}, E_3, and H_3 are constants in the composite (Tong et al., 2008). Thus we can introduce an uniform eigenstrain field

$$\begin{aligned} \varepsilon^* &= \varepsilon_{11}^* = \varepsilon_{22}^* \\ &= (-C_{13}\varepsilon_{33} + e_{31}E_3 + q_{31}H_3)/(C_{11} + C_{12}). \end{aligned} \tag{2.2}$$

Substitution of Eq. (2.2) into Eq. (2.1) yields

$$\begin{aligned} &\sigma_{11} + \sigma_{22} = 2K[(\varepsilon_{11} + \varepsilon_{22}) - 2\varepsilon^*], \\ &\sigma_{22} - \sigma_{11} = 2\mu(\varepsilon_{22} - \varepsilon_{11}), \\ &\sigma_{12} = 2\mu\varepsilon_{12} \end{aligned} \tag{2.3}$$

and

$$\begin{aligned} &\sigma_{33} = C_{13}(\varepsilon_{11} + \varepsilon_{22}) + C_{33}\varepsilon_{33} - e_{33}E_3 - q_{33}H_3, \\ &D_3 = e_{31}(\varepsilon_{11} + \varepsilon_{22}) + e_{33}\varepsilon_{33} + \kappa_{33}E_3 + \lambda_{33}H_3, \\ &B_3 = q_{31}(\varepsilon_{11} + \varepsilon_{22}) + q_{33}\varepsilon_{33} + \lambda_{33}E_3 + \mu_{33}H_3, \end{aligned} \tag{2.4}$$

where $K = (C_{11} + C_{12})/2$ is the in-plane bulk modulus, and $\mu = (C_{11} - C_{12})/2$ is the transverse shear modulus. It is

noted that the in-plane stress–strain fields (2.3) in the piezoelectric–piezomagnetic composite material is the same as that in the corresponding elastic material with an appropriate uniform eigenstrain field ε^* (2.2). Therefore, the multi-field coupled problem is reduced to an equivalent in-plane elastic problem with the eigenstrain ε^*. Once the in-plane strain is determined, the out-of-plane stress, electric displacement, and magnetic flux are also determined through (2.4).

3. Representation of the solution

We follow Kolosov–Muskhelishvili formulae to express the stress via two complex potentials $\varphi(z)$ and $\psi(z)$ as follows (Muskhelishvili, 1975)

$$\begin{aligned}&\sigma_{11}+\sigma_{22}=2[\varphi(z)+\overline{\varphi'(z)}],\\&\sigma_{22}-\sigma_{11}+2i\sigma_{12}=2[\bar{z}\varphi''(z)+\psi'(z)],\end{aligned}\tag{3.1}$$

where the overbar represents the complex conjugate, and the prime denotes differentiation. In these equations, $z=x_1+ix_2$ is complex coordinate of a point (x_1,x_2) in the global Cartesian coordinate system, and $i=\sqrt{-1}$. The displacement $\mathbf{u}$ and resultant stress $\mathbf{F}$ are then obtained as

$$\begin{aligned}&\mathbf{u}=u_1+iu_2=\frac{1}{2\mu}\left[\kappa\varphi(z)-z\overline{\varphi'(z)}-\overline{\psi(z)}\right]+\varepsilon^* z,\\&\mathbf{F}=F_1+iF_2=-i\left[\varphi(z)+z\overline{\varphi'(z)}+\overline{\psi(z)}\right]_{\mathcal{A}}^{\mathcal{B}},\end{aligned}\tag{3.2}$$

where $\kappa=3-4\nu$ in plane strain; $\kappa=(3-\nu)/(1+\nu)$ in plane stress; ν is Poisson's ratio; F_1 and F_2 are the resultant stress components from point $\mathcal{A}$ to point $\mathcal{B}$ along any arc, and $[\cdot]_{\mathcal{A}}^{\mathcal{B}}$ denotes the value difference between two points $\mathcal{A}$ and $\mathcal{B}$.

Further, we assume that the interfaces are perfectly bonded, and therefore the field quantities satisfy

$$\mathbf{u}_m|_{\partial V_p}=\mathbf{u}_i^{(p)}\Big|_{\partial V_p},\quad \mathbf{F}_m|_{\partial V_p}=\mathbf{F}_i^{(p)}\Big|_{\partial V_p},\tag{3.3}$$

where $\partial V_p=a_p e^{i\theta_p}\equiv a_p\sigma_p$, and the subscripts m and i denote the matrix and inclusion, respectively.

Following Buryachenko and Kushch (2006), the general solution for the matrix is the superposition of the external applied field and the disturbances induced by the inclusions. That is,

$$\mathbf{u}_m=\mathbf{u}_{ext}+\sum_{l=1}^{N}\mathbf{u}_m^{(l)},\quad \mathbf{F}_m=\mathbf{F}_{ext}+\sum_{l=1}^{N}\mathbf{F}_m^{(l)},\tag{3.4}$$

where

$$\begin{aligned}&\mathbf{u}_{ext}=\frac{1}{2\mu_m}\left[\kappa_m\varphi_{ext}(z)-z\overline{\varphi'_{ext}(z)}-\overline{\psi_{ext}(z)}\right]+\varepsilon_m^* z,\\&\mathbf{u}_m^{(l)}=\frac{1}{2\mu_l}\left[\kappa_l\varphi_m^{(l)}(z_l)-z_l\overline{\varphi_m^{(l)\prime}(z_l)}-\overline{\psi_m^{(l)}(z_l)}\right],\\&\mathbf{F}_{ext}=\varphi_{ext}(z)+z\overline{\varphi'_{ext}(z)}+\overline{\psi_{ext}(z)},\\&\mathbf{F}_m^{(l)}=\varphi_m^{(l)}(z_l)+z_l\overline{\varphi_m^{(l)\prime}(z_l)}+\overline{\psi_m^{(l)}(z_l)},\end{aligned}\tag{3.5}$$

$z_l=z-Z_l$, and Z_l is the center of the lth inclusion. On the contrary, for the pth inclusion

$$\begin{aligned}&\mathbf{u}_i^{(p)}=\frac{1}{2\mu_p}\left[\kappa_p\varphi_i^{(p)}(z_p)-z_p\overline{\varphi_i^{(p)\prime}(z_p)}-\overline{\psi_i^{(p)}(z_p)}\right]+\varepsilon_p^* z_p,\\&\mathbf{F}_i^{(p)}=\varphi_i^{(p)}(z_p)+z_p\overline{\varphi_i^{(p)\prime}(z_p)}+\overline{\psi_i^{(p)}(z_p)}.\end{aligned}\tag{3.6}$$

We consider a situation where the composite is subjected to a homogeneous remote strain ε_{ij}^0. It follows from $(3.5)_1$ that

$$\varphi_{ext}(z)=\Gamma_\varphi z,\quad \psi_{ext}(z)=\Gamma_\psi z,\tag{3.7}$$

where

$$\Gamma_\varphi=\frac{\mu_m(\varepsilon_{11}^0+\varepsilon_{22}^0)}{\kappa_m-1},\quad \Gamma_\psi=\mu_m(\varepsilon_{22}^0-\varepsilon_{11}^0+2i\varepsilon_{12}^0).\tag{3.8}$$

Similarly if the composite is subjected to a homogeneous remote stress σ_{ij}^0,

$$\Gamma_\varphi=\frac{\sigma_{11}^0+\sigma_{22}^0}{4},\quad \Gamma_\psi=\frac{\sigma_{22}^0-\sigma_{11}^0+2i\sigma_{12}^0}{2}.\tag{3.9}$$

In addition, the potential fields for the pth cylinder and its matrix can be expanded as

$$\varphi_i^{(p)}(z_p)=\sum_{n=0}^{\infty}C_n^{(p)}z_p^n,\quad \psi_i^{(p)}(z_p)=\sum_{n=0}^{\infty}D_n^{(p)}z_p^n\tag{3.10}$$

for the inclusion, and

$$\varphi_m^{(l)}(z_l)=\sum_{n=1}^{\infty}A_n^{(l)}z_l^{-n},\quad \psi_m^{(l)}(z_l)=\sum_{n=1}^{\infty}B_n^{(l)}z_l^{-n}\tag{3.11}$$

for the matrix. Here the coefficients $A_n^{(l)}$, $B_n^{(l)}$, $C_n^{(l)}$ and $D_n^{(l)}$ are some unknowns to be determined. The superscript $p(l)$ indicates that the fields are expanded with respect to the pth (lth) cylinder's center Z_p (Z_l).

To proceed, we shift the origin of the expansions to a fixed point, say Z_p. For point z satisfying the inequality $|z_p|<|Z_p-Z_l|$, we can expand the term z_l^{-n} using the binomial theorem as

$$z_l^{-n}=\sum_{s=0}^{\infty}(-1)^s\binom{n+s-1}{s}(Z_p-Z_l)^{-n-s}z_p^s\equiv\sum_{s=0}^{\infty}\mathcal{L}_{ns}^{pl}z_p^s.\tag{3.12}$$

Introducing (3.11) and (3.12) into (3.4), we have the expansions

$$\sum_{l=1}^{N}\varphi_m^{(l)}(z_l)=\sum_{n=1}^{\infty}A_n^{(p)}z_p^{-n}+\sum_{s=0}^{\infty}A_{-s}^{(p)}z_p^s,\tag{3.13}$$

$$\sum_{l=1}^{N}\psi_m^{(l)}(z_l)=\sum_{n=1}^{\infty}B_n^{(p)}z_p^{-n}+\sum_{s=0}^{\infty}B_{-s}^{(p)}z_p^s\tag{3.14}$$

and

$$\sum_{l=1}^{N}z_l\overline{\varphi_m^{(l)\prime}(z_l)}=z_p\left[-\sum_{n=1}^{\infty}n\overline{A_n^{(p)}z_p^{-n-1}}+\sum_{s=0}^{\infty}s\overline{A_{-s}^{(p)}z_p^{s-1}}\right]-\sum_{s=0}^{\infty}\overline{\mathbb{A}_{-s}^{(p)}z_p^s},\tag{3.15}$$

which are valid for the domain

$$|z_p|\leqslant\min(|Z_p-Z_l|),\quad \text{for } l=1,2,\ldots,N,\quad l\neq p.\tag{3.16}$$

Here

$$A_{-s}^{(p)} \equiv \sum_{l\neq p}^{N}\sum_{n=1}^{\infty} A_n^{(l)}\mathcal{L}_{ns}^{pl}, \quad B_{-s}^{(p)} \equiv \sum_{l\neq p}^{N}\sum_{n=1}^{\infty} B_n^{(l)}\mathcal{L}_{ns}^{pl},$$
$$\mathbb{A}_{-s}^{(p)} \equiv \sum_{l\neq p}^{N}\sum_{n=1}^{\infty} A_n^{(l)}\mathcal{L}_{ns}^{pl}(n+s)\frac{|Z_p-Z_l|^2}{(Z_p-Z_l)^2}. \tag{3.17}$$

Substituting (3.10), (3.11) and (3.13)–(3.15) into the interface conditions (3.3), we obtain

$$\begin{aligned}
&\frac{1}{2\mu_m}\Bigg\{\kappa_m\left[\Gamma_\varphi(a_p\sigma_p+Z_p)+\sum_{s=1}^{\infty}A_s^{(p)}a_p^{-s}\sigma_p^{-s}+\sum_{s=0}^{\infty}A_{-s}^{(p)}a_p^{s}\sigma_p^{s}\right]\\
&-\overline{\Gamma_\varphi}(a_p\sigma_p+Z_p)\\
&-a_p\sigma_p\left(-\sum_{s=1}^{\infty}s\overline{A_s^{(p)}}a_p^{-s-1}\sigma_p^{s+1}+\sum_{s=0}^{\infty}s\overline{A_{-s}^{(p)}}a_p^{s-1}\sigma_p^{-s+1}\right)\\
&+\sum_{s=0}^{\infty}\overline{\mathbb{A}_{-s}^{(p)}}a_p^{s}\sigma_p^{-s}-\overline{\Gamma_\psi}\left(a_p^{-1}\sigma_p+\overline{Z_p}\right)-\sum_{s=1}^{\infty}\overline{B_s^{(p)}}a_p^{-s}\sigma_p\\
&-\sum_{s=0}^{\infty}\overline{B_{-s}^{(p)}}a_p^{s}\sigma_p^{-s}\Bigg\}+\varepsilon_m^*(a_p\sigma_p+Z_p)\\
&=\frac{1}{2\mu_p}\left[\kappa_p\sum_{s=0}^{\infty}C_s^{(p)}a_p^{s}\sigma_p^{s}-a_p\sigma_p\sum_{s=0}^{\infty}s\overline{C_s^{(p)}}a_p^{s-1}\sigma_p^{-s+1}-\sum_{s=0}^{\infty}\overline{D_s^{(p)}}a_p^{s}\sigma_p^{-s}\right]\\
&+\varepsilon_p^*a_p\sigma_p
\end{aligned} \tag{3.18}$$

and

$$\begin{aligned}
&\Gamma_\varphi(a_p\sigma_p+Z_p)+\sum_{s=1}^{\infty}A_s^{(p)}a_p^{-s}\sigma_p^{-s}+\sum_{s=0}^{\infty}A_{-s}^{(p)}a_p^{s}\sigma_p^{s}\\
&+\overline{\Gamma_\varphi}(a_p\sigma_p+Z_p)\\
&+a_p\sigma_p\left(-\sum_{s=1}^{\infty}s\overline{A_s^{(p)}}a_p^{-s-1}\sigma_p^{s+1}+\sum_{s=0}^{\infty}s\overline{A_{-s}^{(p)}}a_p^{s-1}\sigma_p^{-s+1}\right)\\
&-\sum_{s=0}^{\infty}\overline{\mathbb{A}_{-s}^{(p)}}a_p^{s}\sigma_p^{-s}+\overline{\Gamma_\psi}(a_p\sigma_p^{-1}+\overline{Z_p})+\sum_{s=1}^{\infty}\overline{B_s^{(p)}}a_p^{-s}\sigma_p^{s}\\
&+\sum_{s=0}^{\infty}\overline{B_{-s}^{(p)}}a_p^{s}\sigma_p^{-s}\\
&=\sum_{s=0}^{\infty}C_s^{(p)}a_p^{s}\sigma_p^{s}+a_p\sigma_p\sum_{s=0}^{\infty}s\overline{C_s^{(p)}}a_p^{s-1}\sigma_p^{-s+1}\\
&+\sum_{s=0}^{\infty}\overline{D_s^{(p)}}a_p^{s}\sigma_p^{-s}.
\end{aligned} \tag{3.19}$$

Equating the coefficients of σ_p^s and σ_p^{-s} of (3.18) and (3.19) gives

$$\begin{aligned}
&\frac{1}{2\mu_m}\Big\{\left[(\kappa_m-1)\Gamma_\varphi-\overline{A_{-1}^{(p)}}\right]a_p\delta_{s1}\\
&+\left[(\kappa_m-1)\Gamma_\varphi Z_p-\overline{\Gamma_\psi Z_p}-2\overline{A_{-2}^{(p)}}a_p^2+\overline{\mathbb{A}_{-0}^{(p)}}-\overline{B_{-0}^{(p)}}\right]\delta_{s0}\\
&+\kappa_mA_{-s}^{(p)}a_p^{s}+(s-2)\overline{A_{s-2}^{(p)}}a_p^{-s+2}H(s-3)-\overline{B_s^{(p)}}a_p^{-s}H(s-1)\Big\}\\
&+\varepsilon_m^*(a_p\delta_{s1}+Z_p\delta_{s0})\\
&=\frac{1}{2\mu_p}\left[\kappa_pC_s^{(p)}a_p^{s}-\overline{C_1^{(p)}}a_p\delta_{s1}-(2\overline{C_2^{(p)}}a_p^2+\overline{D_0^{(p)}})\delta_{s0}\right]\\
&+\varepsilon_p^*a_p\delta_{s1},\quad s\geqslant 0,
\end{aligned} \tag{3.20}$$

$$\begin{aligned}
&-\overline{\Gamma_\psi}a_p\delta_{s1}+\kappa_mA_s^{(p)}a_p^{-s}-(s+2)\overline{A_{-(s+2)}^{(p)}}a_p^{s+2}+\overline{\mathbb{A}_{-s}^{(p)}}a_p^{s}-\overline{B_{-s}^{(p)}}a_p^{s}\\
&=-\frac{\mu_m}{\mu_p}\left[(s+2)\overline{C_{s+2}^{(p)}}a_p^{s+2}+\overline{D_s^{(p)}}a_p^{s}\right],\quad s\geqslant 1
\end{aligned} \tag{3.21}$$

and

$$\begin{aligned}
&(2\Gamma_\varphi+\overline{A_{-1}^{(p)}})a_p\delta_{s1}+(2\Gamma_\varphi Z_p+\overline{\Gamma_\psi Z_p}+2\overline{A_{-2}^{(p)}}a_p^2-\overline{\mathbb{A}_{-0}^{(p)}}+\overline{B_{-0}^{(p)}})\delta_{s0}\\
&+A_{-s}^{(p)}a_p^{(s)}-(s-2)\overline{A_{s-2}^{(p)}}a_p^{-s+2}H(s-3)+\overline{B_s^{(p)}}a_p^{-s}H(s-1)\\
&=C_s^{(p)}a_p^{s}+\overline{C_1^{(p)}}a_p\delta_{s1}+(2\overline{C_2^{(p)}}a_p^2+\overline{D_0^{(p)}})\delta_{s0},\quad s\geqslant 0,
\end{aligned} \tag{3.22}$$

$$\begin{aligned}
&\overline{\Gamma_\psi}a_p\delta_{s1}+A_s^{(p)}a_p^{-s}+(s+2)\overline{A_{-(s+2)}^{(p)}}a_p^{s+2}-\overline{\mathbb{A}_{-s}^{(p)}}a_p^{s}+\overline{B_{-s}^{(p)}}a_p^{s}\\
&=(s+2)\overline{C_{s+2}^{(p)}}a_p^{s+2}+\overline{D_s^{(p)}}a_p^{s},\quad s\geqslant 1,
\end{aligned} \tag{3.23}$$

where δ_{ij} is the Kronecker delta and $H(\cdot)$ is the unit step function.

After some algebra, Eqs. (3.20)–(3.23) can be arranged as

$$\begin{aligned}
&\Lambda_1^{(p)}A_s^{(p)}a_p^{-2s}+(s+2)\overline{A_{-(s+2)}^{(p)}}a_p^2-\overline{\mathbb{A}_{-s}^{(p)}}+\overline{B_{-s}^{(p)}}\\
&=-\overline{\Gamma_\psi}\delta_{s1},\quad s\geqslant 1,
\end{aligned} \tag{3.24}$$

$$\Lambda_3^{(p)}\overline{B_1^{(p)}}a_p^{-2}+\mathrm{Re}\overline{A_{-1}^{(p)}}=\Lambda_4^{(p)}-\Gamma_\varphi,\quad s=1, \tag{3.25}$$

$$\overline{A_{-s}^{(p)}}+\Lambda_2^{(p)}\left[(s-2)\overline{A_{s-2}^{(p)}}a_p^{-2s+2}-\overline{B_s^{(p)}}a_p^{-2s}\right]=0,\quad s\geqslant 2 \tag{3.26}$$

and

$$\begin{aligned}
C_0^{(p)}&=\frac{\gamma_p}{\kappa_p+1}\left[\left(\gamma_p^{-1}+\kappa_m\right)\left(\Gamma_\varphi Z_p+A_{-0}^{(p)}\right)+2\mu_mZ_p\varepsilon_m^*\right]\\
&+\frac{1-\gamma_p}{\kappa_p+1}\left(\overline{\Gamma_\varphi}Z_p+\overline{\Gamma_\psi Z_p}+2\overline{A_{-2}^{(p)}}a_p^2-\overline{\mathbb{A}_{-0}^{(p)}}+\overline{B_{-0}^{(p)}}\right),
\end{aligned} \tag{3.27}$$

$$C_1^{(p)}=\frac{\gamma_p}{2\gamma_p+\kappa_p-1}\mathrm{Re}\Pi+\mathrm{i}\frac{\gamma_p}{\kappa_p+1}\mathrm{Im}\Pi, \tag{3.28}$$

$$C_s^{(p)}=A_{-s}^{(p)}-(s-2)\overline{A_{s-2}^{(p)}}a_p^{-2s+2}+\overline{B_s^{(p)}}a_p^{-2s},\quad s\geqslant 2, \tag{3.29}$$

$$\begin{aligned}
D_0^{(p)}&=2\Gamma_\varphi\overline{Z_p}+\Gamma_\psi Z_p+\overline{A_{-0}^{(p)}}+B_{-0}^{(p)}-\overline{C_0^{(p)}}-\mathbb{A}_{-0}^{(p)}\\
&+2\left(A_{-2}^{(p)}-C_2^{(p)}\right)a_p^2,
\end{aligned} \tag{3.30}$$

$$\begin{aligned}
D_s^{(p)}&=\Gamma_\psi\delta_{s1}+\overline{A_s^{(p)}}a_p^{-2s}+(s+2)A_{-(s+2)}^{(p)}a_p^2-\mathbb{A}_{-s}^{(p)}\\
&+B_{-s}^{(p)}-(s+2)C_{s+2}^{(p)}a_p^2
\end{aligned} \tag{3.31}$$

for $s\geqslant 1$. Here

$$\begin{aligned}
&\gamma_p=\mu_p/\mu_m,\quad \Pi=(\kappa_m+1)\left(\Gamma_\varphi+A_{-1}^{(p)}\right)+2\mu_m\left(\varepsilon_m^*-\varepsilon_p^*\right),\\
&\Lambda_1^{(p)}=\frac{1+\kappa_m\gamma_p}{1-\gamma_p},\quad \Lambda_2^{(p)}=\frac{\gamma_p+\kappa_p}{\kappa_m\gamma_p-\kappa_p},\\
&\Lambda_3^{(p)}=\frac{2\gamma_p+\kappa_p-1}{2\left[\kappa_p-1-\gamma_p(\kappa_m-1)\right]},\quad \Lambda_4^{(p)}=\frac{2\mu_m\gamma_p(\varepsilon_m^*-\varepsilon_p^*)}{\kappa_p-1-\gamma_p(\kappa_m-1)}.
\end{aligned} \tag{3.32}$$

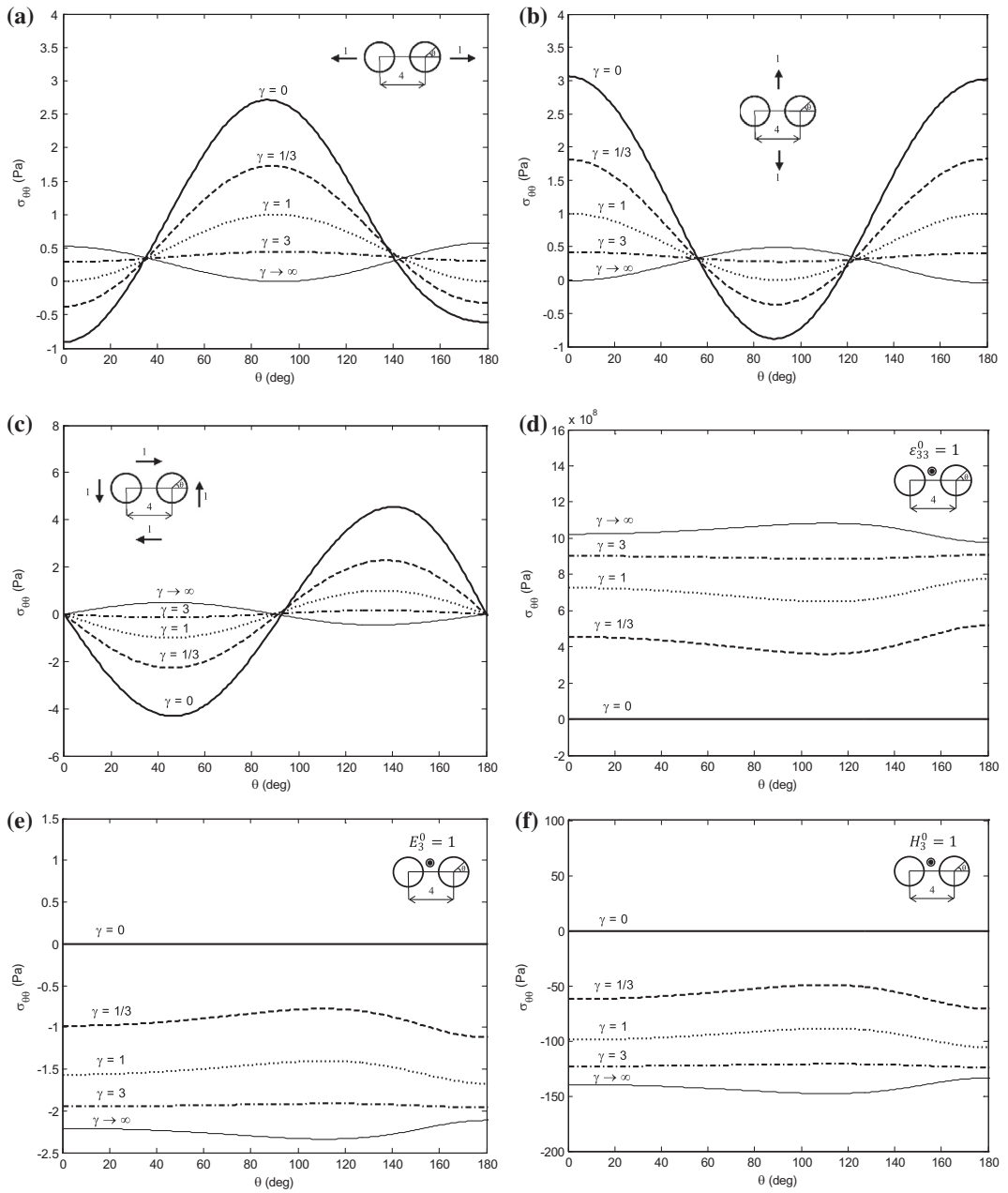

Fig. 2. The hoop stress $\sigma_{\theta\theta}$ in the matrix along the interface for discrete values of $\gamma = \mu_i/\mu_m$ under six different remote loading cases (two PE inclusions in a PM matrix): (a) uniform tension $\sigma^0_{11} = 1$, (b) uniform tension $\sigma^0_{22} = 1$, (c) pure shear $\sigma^0_{12} = 1$, (d) uniform vertical strain $\varepsilon^0_{33} = 1$, (e) uniform transverse electric field $E^0_3 = 1$ and (f) uniform transverse magnetic field $H^0_3 = 1$.

Eqs. (3.24)–(3.26) and their conjugates constitute an infinite set of linear algebraic equations. Upon appropriate truncations of the expansion terms, we can determine the expansion coefficients $A^{(p)}_n$ and $B^{(p)}_n$. Substituting them back to (3.27)–(3.31), we can determine the remaining coefficients $C^{(p)}_n$ and $D^{(p)}_n$. After they are determined, all the complex potentials of the matrix and inclusions are known, and then all the field variables can be easily obtained from Eqs. (3.1) and (3.2). For instance, the stress fields in the polar coordinate are given by the transformation

$$\begin{aligned}
\sigma_{rr} &= \frac{\sigma_{11}+\sigma_{22}}{2} + \frac{\sigma_{11}-\sigma_{22}}{2}\cos 2\theta + \sigma_{12}\sin 2\theta,\\
\sigma_{\theta\theta} &= \frac{\sigma_{11}+\sigma_{22}}{2} - \frac{\sigma_{11}-\sigma_{22}}{2}\cos 2\theta - \sigma_{12}\sin 2\theta,\\
\sigma_{r\theta} &= -\frac{\sigma_{11}-\sigma_{22}}{2}\sin 2\theta + \sigma_{12}\cos 2\theta. \qquad (3.33)
\end{aligned}$$

4. Numerical results and discussion

Below we perform a numerical computation for stress and displacement fields of composites of various

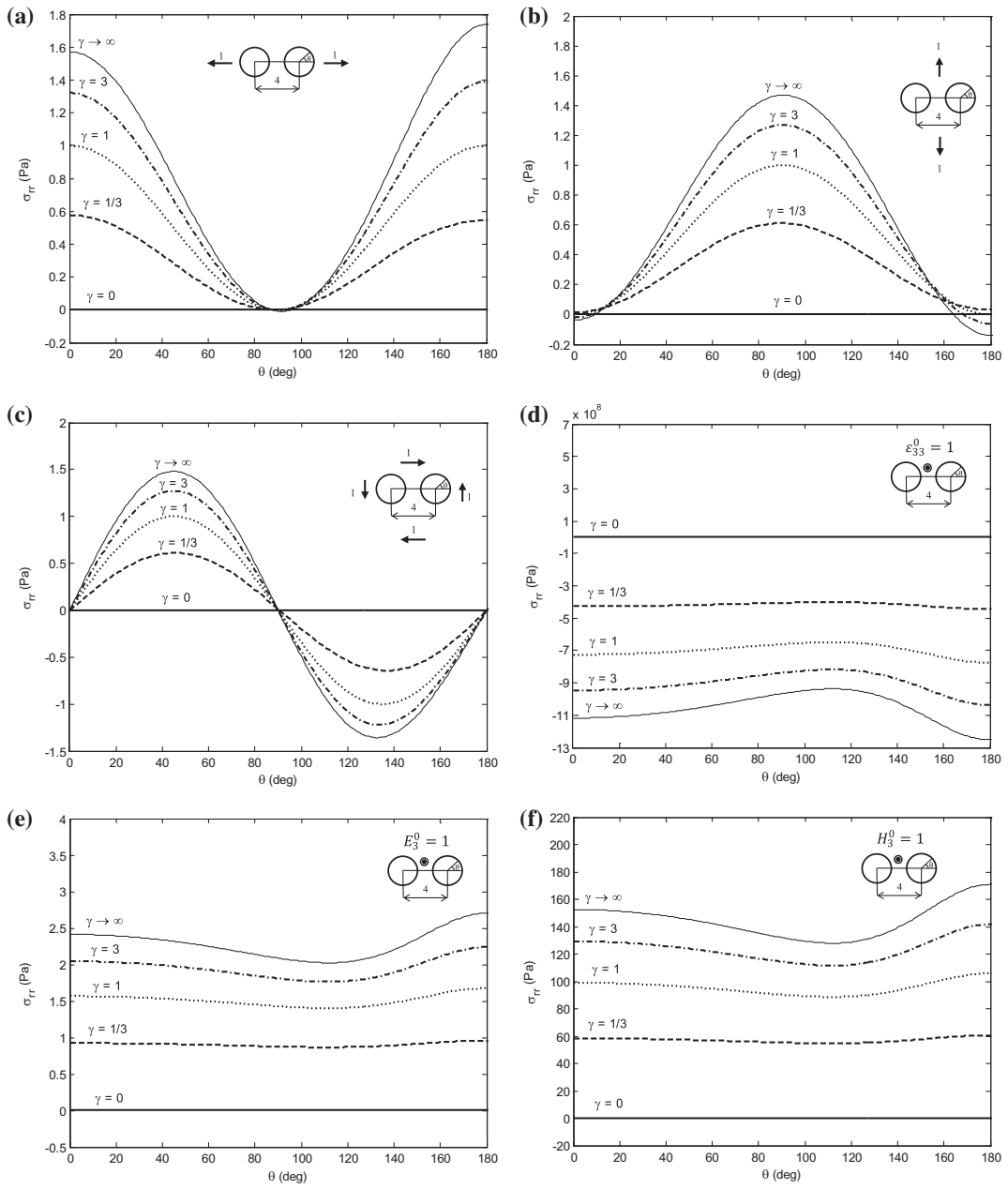

Fig. 3. The normal contact stress σ_{rr} in the matrix along the interface for discrete values of $\gamma = \mu_i/\mu_m$ under six different remote loading cases (two PE inclusions in a PM matrix): (a) uniform tension $\sigma^0_{11} = 1$, (b) uniform tension $\sigma^0_{22} = 1$, (c) pure shear $\sigma^0_{12} = 1$, (d) uniform vertical strain $\varepsilon^0_{33} = 1$, (e) uniform transverse electric field $E^0_3 = 1$ and (f) uniform transverse magnetic field $H^0_3 = 1$.

remote loadings. The numerical calculations are first verified with the analytical solution for a composite of a piezoelectric inclusion in an elastic matrix. Our results of stress distributions agree very well with those of the solution proposed by Xiao and Bai (1999). Next we consider the particular case of a piezoelectric–piezomagnetic composite including a single inclusion with the center O, i.e. $Z_1 = 0$. The only non-zero coefficients are

$$
\begin{aligned}
A_1 &= -\Lambda_1^{-1}\overline{\Gamma_\psi}a^2,\\
B_1 &= 2a^2\left[\frac{(\kappa_m+1)\Gamma_\varphi + 2\mu_m\left(\varepsilon^*_m-\varepsilon^*_i\right)}{2+\frac{\mu_m}{\mu_i}(\kappa_i-1)} - \Gamma_\varphi\right],\\
B_3 &= -\Lambda_1^{-1}\overline{\Gamma_\psi}a^4,\\
C_1 &= \frac{(\kappa_m+1)\Gamma_\varphi + 2\mu_m\left(\varepsilon^*_m-\varepsilon^*_i\right)}{2+\frac{\mu_m}{\mu_i}(\kappa_i-1)},\\
D_1 &= (1-\Lambda_1^{-1})\Gamma_\psi.
\end{aligned}
\tag{4.1}
$$

Therefore, the complex potentials

$$\varphi_m(z) = A_1 z^{-1},$$
$$\psi_m(z) = B_1 z^{-1} + B_3 z^{-3} \tag{4.2}$$

for the matrix, and

$$\varphi_i(z) = C_1 z,$$
$$\psi_i(z) = D_1 z \tag{4.3}$$

for the inclusion.

Substitutions of (4.2) and (4.3) into Eq. $(3.1)_1$, we obtain the stress field in the fiber

$$(\sigma_{11} + \sigma_{22})_i = 4\frac{(\kappa_m + 1)\Gamma_\varphi + 2\mu_m(\varepsilon_m^* - \varepsilon_i^*)}{2 + \frac{\mu_m}{\mu_i}(\kappa_i - 1)}, \tag{4.4}$$

which covers the known result by Tong et al. (2008).

We now turn to the case of two inclusions of unit radius and with identical material properties placed on the x_1-axis and $|Z_1 - Z_2| = 4$. The inclusion is piezoelectric (PE), while the matrix is piezomagnetic (PM). A state of plane stress is assumed. The hoop stress is presented in Fig. 2 for six different remote loading cases. Poisson's ratio for both the inclusions and matrix is the same with $\nu_i = \nu_m = 1/3$, but the shear modulus of the inclusions is different from that of the matrix. Circumferential stresses $\sigma_{\theta\theta}$ are plotted for $\gamma = \mu_i/\mu_m = 0,\ 1/3,\ 1,\ 3,\ \infty$. The remaining material constants are: $e_{31} = -4.32\ \mathrm{C/m^2}$, $e_{33} = 18.6\ \mathrm{C/m^2}$, $\kappa_{33} = 11.8 \times 10^{-9}\ \mathrm{C^2/Nm^2}$, $\mu_{33} = 10 \times 10^{-6}\ \mathrm{Ns^2/C^2}$ for the PE phase, and $q_{31} = 580.3\ \mathrm{N/Am}$, $q_{33} = 699.7\ \mathrm{N/Am}$, $\kappa_{33} = 0.093 \times 10^{-9}\ \mathrm{C^2/Nm^2}$, $\mu_{33} = 157 \times 10^{-6}\ \mathrm{Ns^2/C^2}$ for the PM phase. The results in Fig. 2(a)–(c) agree within the plotting accuracy with results from Yu and Sendeckyj (1974) and Mogilevskaya and Crouch (2001) for the pure elastic problem. This is because $\varepsilon^* = 0$ for these cases. The loading case for vertical strain and transverse electromagnetic fields (Fig. 2(d)–(f)) is new. It is interesting to observe that, in contrast to the stress concentration around the holes subjected to in-plane loadings, the hoop stress is zero around the holes subjected to the external applied vertical strain and transverse electromagnetic fields. On the other hand, there is no concentration for the normal contact stress σ_{rr} around the holes under all kinds of remote loadings (Fig. 3). Further, the stress concentration in a multiferroic composite may aggravate or alleviate by adjusting the magnitude and sign of various loading combinations.

Fig. 4 shows the hoop stress in the matrix along the interface under an uniform remote tension $\sigma_{11}^0 = 1$ for a PM matrix containing three PE inclusions. The material properties are the same as those for the two-inclusion case. Again, the results agree within the plotting accuracy with the result from Mogilevskaya and Crouch (2001) by the Galerkin boundary integral method for the pure elastic problem.

Finally, in Fig. 5 we demonstrate the displacement contours for a PM matrix containing five PE inclusions under an uniform remote tension $\sigma_{11}^0 = 1$. Each of the inclusions has different material properties and radii ($\mu_1/\mu_m = 4,\ \mu_2/\mu_m = 6,\ \mu_3/\mu_m = 8,\ \mu_4/\mu_m = 10,\ \mu_5/\mu_m = 12.\ a_1 = 1.5,\ a_2 = 1.25,\ a_3 = 1,\ a_4 = 0.75,\ a_5 = 0.5.\ O_1 =$

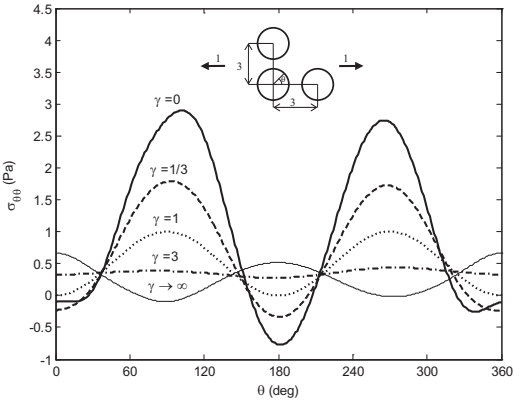

Fig. 4. The hoop stress $\sigma_{\theta\theta}$ in the matrix along the interface for discrete values of $\gamma = \mu_i/\mu_m$ under uniform tension $\sigma_{11}^0 = 1$ (three PE inclusions in a PM matrix).

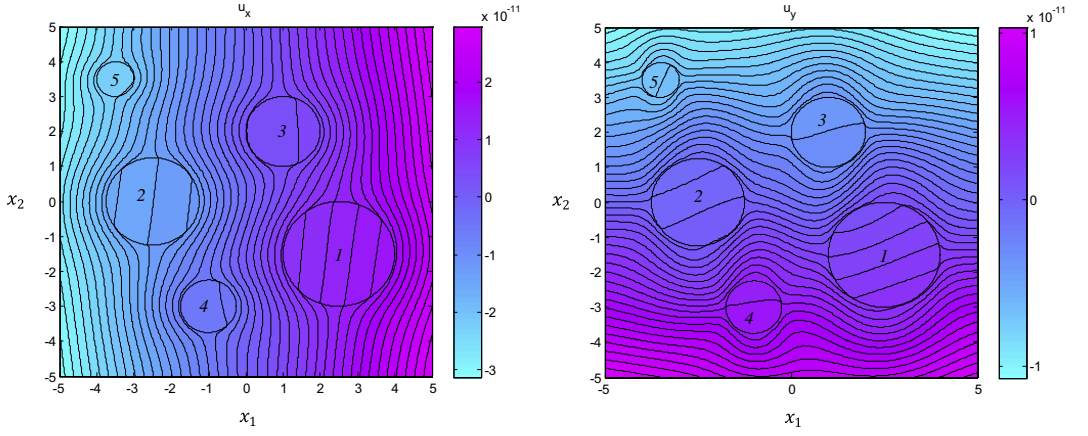

Fig. 5. The displacement contours for a PM matrix containing five PE inclusions under an uniform remote tension $\sigma_{11}^0 = 1$. Phase properties are $\mu_1/\mu_m = 4,\ \mu_2/\mu_m = 6,\ \mu_3/\mu_m = 8,\ \mu_4/\mu_m = 10,\ \mu_5/\mu_m = 12$. The radii are $a_1 = 1.5,\ a_2 = 1.25,\ a_3 = 1,\ a_4 = 0.75,\ a_5 = 0.5$. The centers of the inclusions locate at $O_1 = (2.5, -1.5),\ O_2 = (-2.5, 0),\ O_3 = (1, 2),\ O_4 = (-1, -3)$, and $O_5 = (-3.5, 3.5)$, respectively.

$(2.5,-1.5)$, $O_2=(-2.5,0)$, $O_3=(1,2)$, $O_4=(-1,-3)$, $O_5=(-3.5,3.5)$. The remaining material properties are the same as those for the two-inclusion case). We observe that, in contrast to the generalized anti-plane case (Kuo and Bhattacharya, 2013) the displacement fields inside the inclusions are nonlinear with respect to z. Thus the higher-order terms play an important role in the in-plan deformation.

5. Concluding remarks

In summary, we have extended Muskhelishvili's formulation on an elastic composite with circular boundaries to a magneto-electro-elastic composite consisting of multiple cylinders under generalized plane strain with transverse electromagnetic intensities. We reduce the multi-field coupling problem to an equivalent in-plane elasticity problem by introducing an uniform eigenstrain corresponding to the magneto-electro-elastic effect. The admissible potentials for the inclusions and matrix are calculated within sufficient accuracy for several configuration under different loading cases. Numerical results are compared with the previous known solutions and are shown in good agreement. It is observed that, in contrast to the stress concentration around the holes subjected to in-plane loadings, the stress is zero around the holes under the external applied vertical strain or transverse electromagnetic fields. In addition, the stress concentration in a piezoelectric–piezomagnetic composite may aggravate or alleviate by adjusting the magnitude and sign of various loading combinations.

Acknowledgment

This work was supported by the National Science Council Taiwan, under Contract No. NSC 102-3332-E-009-087.

References

Aboudi, J., 2001. Micromechanical analysis of fully coupled electro-magneto-thermo-elastic multiphase composites. Smart Mater. Struct. 10, 867–877.
Astrov, D.N., 1960. The magnetoelectric effect in antiferromagnetics. Sov. Phys.-JETP 11, 708.
Benveniste, Y., 1995. Magnetoelectric effect in fibrous composites with piezoelectric and piezomagnetic phases. Phys. Rev. B 51, 16424–16427.
Bichurin, M.I., Petrov, V.M., Kiliba, Yu.V., Srinivasan, G., 2002. Magnetic and magnetoelectric susceptibilities of a ferroelectric/ferromagnetic composite at microwave frequencies. Phys. Rev. B 66, 134404.
Buryachenko, V.A., Kushch, V.I., 2006. Effective transverse elastic moduli of composites at non-dilute concentration of a random field of aligned fibers. Z. Angew. Math. Phys. 57, 491–505.
Camacho-Montes, H., Sabina, F.J., Bravo-Castillero, J., Guinovart-Díaz, R., Rodríguez-Ramos, R., 2009. Magnetoelectric coupling and cross-property connections in a square array of a binary composite. Int. J. Eng. Sci. 47, 294–312.
Fiebig, M., 2005. Revival of the magnetoelectric effect. J. Phys. D: Appl. Phys. 38, R123–R152.
Huang, J.H., Kuo, W.-S., 1997. The analysis of piezoelectric/piezomagnetic composite materials containing ellipsoidal inclusions. J. Appl. Phys. 81, 1378–1386.
Kuo, H.-Y., 2011. Multicoated elliptic fibrous composites of piezoelectric and piezomagnetic phases. Int. J. Eng. Sci. 49, 561–575.
Kuo, H.-Y., Bhattacharya, K., 2013. Fibrous composites of piezoelectric and piezomagnetic phases. Mech. Mater. 60, 159–170.
Kuo, H.-Y., Pan, E., 2011. Effective magnetoelectric effect in multicoated circular fibrous multiferroic composites. J. Appl. Phys. 109, 104901.
Kuo, H.-Y., Slinger, A., Bhattacharya, K., 2010. Optimization of magnetoelectricity in piezoelectric–magnetostrictive bilayers. Smart Mater. Struct. 19, 125010.
Kushch, V.I., Shmegera, S.V., Mishnaevsky Jr., L., 2008. Meso cell model of fiber reinforced composite: interface stress statistics and debonding paths. Int. J. Solids Struct. 45, 2758–2784.
Landau, L.D., Lifshitz, E.M., 1984. Electrodynamics of Continuous Media. Pergamon Press, New York, p. 119.
Lee, J., Boyd IV, J.G., Lagoudas, D.C., 2005. Effective properties of three-phase electro-magneto-elastic composites. Int. J. Eng. Sci. 43, 790–825.
Li, J.Y., Dunn, M.L., 1998. Anisotropic coupled-field inclusion and inhomogeneity problems. Philos. Mag. A 77, 1341–1350.
Liu, L.P., Kuo, H.-Y., 2012. Closed-form solutions to the effective properties of fibrous magnetoelectric composites and their applications. Int. J. Solids Struct. 49, 3055–3062.
Liu, G., Nan, C.-W., Cai, N., Lin, Y., 2004. Dependence of giant magnetoelectric effect on interfacial bonding for multiferroic laminate composites of rare-earth-iron alloys and lead–zirconate–titanate. J. Appl. Phys. 95, 2660–2664.
McPhedran, R.C., Movchan, A.B., 1994. The Rayleigh multiple method for linear elasticity. J. Mech. Phys. Solids 42, 711–727.
Mogilevskaya, S.G., Crouch, S.L., 2001. A Galerkin boundary integral method for multiple circular elastic inclusions. Int. J. Numer. Methods Eng. 52, 1069–1106.
Muskhelishvili, N.I., 1975. Some Basic Problems of the Mathematical Theory of Elasticity. Noordhoff, Leyden, The Netherlands.
Nan, C.-W., 1994. Magnetoelectric effect in composites of piezoelectric and piezomagnetic phases. Phys. Rev. B 50, 6082–6088.
Nan, C.-W., Bichurin, M.I., Dong, S., woehland, D., Srinivasan, G., 2008. Multiferroic magnetoelectric composites: Historical perspective, status, and future directions. J. Appl. Phys. 103, 031101.
Rado, G.T., Folen, V.J., 1961. Observation of the magnetically induced magnetoelectric effect and evidence for antiferromagnetic domains. Phys. Rev. Lett. 7, 310.
Spaldin, N.A., Fiebig, M., 2005. The Renaissance of magnetoelectric multiferroic. Science 309, 391–392.
Srinivas, S., Li, J.Y., 2005. The effective magnetoelectric coefficients of polycrystalline multiferroic composites. Acta Mater. 53, 4135–4142.
Tong, Z.H., Lo, S.H., Jiang, C.P., Cheung, Y.K., 2008. An exact for the three-phase thermo-electro-magneto-elastic cylinder model and its application to piezoelectric–magnetic fiber composites. Int. J. Solids Struct. 45, 5205–5219.
Xiao, Z.M., Bai, J., 1999. On piezoelectric inhomogeneity related problem – Part I: A close-form solution for the stress field outside a circular piezoelectric inhomogeneity. Int. J. Eng. Sci. 37, 945–959.
Yang, B.-H., Gao, C.-F., 2010. Plane problems of multiple piezoelectric inclusions in a non-piezoelectric matrix. Int. J. Eng. Sci. 48, 518–528.
Yu, I.-W., Sendeckyj, G.P., 1974. Multiple circular inclusion problems in plane elastostatics. J. Appl. Mech. 41, 215–221.